

Hydrogen-Induced Rupture of Strained Si—O Bonds in Amorphous Silicon Dioxide

Al-Moatasem El-Sayed,^{1,*} Matthew B. Watkins,^{1,†} Tibor Grasser,^{2,‡} Valery V. Afanas'ev,^{3,§} and Alexander L. Shluger^{1,¶}

¹*Department of Physics and Astronomy and London Centre for Nanotechnology,
University College London, Gower Street, London WC1E 6BT, United Kingdom*

²*Institute for Microelectronics, Technische Universität Wien, A-1040 Vienna, Austria*

³*Department of Physics, University of Leuven, Celestijnenlaan 200D, 3001 Leuven, Belgium*

(Received 2 November 2014; published 18 March 2015)

Using *ab initio* modeling we demonstrate that H atoms can break strained Si—O bonds in continuous amorphous silicon dioxide (*a*-SiO₂) networks, resulting in a new defect consisting of a threefold-coordinated Si atom with an unpaired electron facing a hydroxyl group, adding to the density of dangling bond defects, such as *E'* centers. The energy barriers to form this defect from interstitial H atoms range between 0.5 and 1.3 eV. This discovery of unexpected reactivity of atomic hydrogen may have significant implications for our understanding of processes in silica glass and nanoscaled silica, e.g., in porous low-permittivity insulators, and strained variants of *a*-SiO₂.

DOI: 10.1103/PhysRevLett.114.115503

PACS numbers: 61.72.-y, 71.15.Mb, 71.55.Jv

The interaction of hydrogen with wide-band-gap oxides and minerals is important for many applications and has been the subject of a number of experimental and theoretical studies (see Refs. [1–7], to mention a few). Among these oxides, quartz and amorphous silicon dioxide (*a*-SiO₂) occupy a very prominent place due to their abundance and fundamental and technological importance. Hydrogen, in its more prevalent forms (H₂ and water), is known to induce hydrolytic weakening of quartz and minerals [8] and degradation phenomena in optical fibers [9] and in SiO₂-insulated electronic devices. These effects can be facilitated by irradiation [10–12], as well as electron injection [13] and lead to bias-temperature instabilities [14,15]. However, the involvement of atomic hydrogen in silica network degradation mechanisms is still poorly understood.

A supply of hydrogen (H₂ or forming gas) during thermal treatment or irradiation may lead to formation of additional densities of intrinsic defects, as revealed by electron paramagnetic resonance (EPR) studies of defects in various forms of *a*-SiO₂ [15]. These densities may by far exceed the density of the same defects in identical *a*-SiO₂ films processed in the absence of hydrogen [16]. The additional defects are predominantly Si dangling bonds in the bulk of *a*-SiO₂ [17] or at the Si/SiO₂ interface [18,19], suggesting that Si—O bond rupture occurs in the initially defect-free *a*-SiO₂ network as well as at the Si/*a*-SiO₂ interface. Accumulation of hydrogen inside the *a*-SiO₂ layer has been revealed by a variety of methods (see Ref. [20] and references therein), firmly supporting this conjecture and indicating passivation of the broken bonds by hydrogen [20,21] as well as enhanced mobility of O atoms in the network [22,23]. Although the Si—O bond rupture was initially correlated to the presence of protonic species [24,25] formed by hole trapping [26] or by hydrogen ionization at the Si/SiO₂ interface [27], the involvement

of H⁰ must be considered as well since atomic hydrogen is by far more abundant than protons in processed *a*-SiO₂. For example, *a*-SiO₂ layers are inevitably exposed to H⁰ during processing of microelectronic devices in H-containing environments ranging from the annealing, deposition, and patterning to electrical stressing and irradiation [20].

A clear experimental evidence of silica network damage by atomic hydrogen has been demonstrated by EPR analysis of another form of *a*-SiO₂, the OH-rich synthetic silica widely used in UV optics. Under ArF or F₂ laser irradiation, high concentrations of H⁰ are photolytically generated. Atomic hydrogen is found to easily diffuse through the silica network with activation energies of 0.1–0.2 eV [4,5], but a number of H-related defects have also been detected after irradiation [28–31]. In particular, a 0.08 mT doublet due to proton hyperfine splitting has been assigned to a Si dangling bond coordinated by two bridging oxygens and an OH group. This center is thought to result from the interaction of H⁰ with electronically excited strained Si—O bonds [30]. Strained Si—O bonds in amorphous silica, that is those bonds whose length deviates strongly from the crystalline equilibrium value of 1.61 Å, have been the focus of many other studies due to their relatively high reactivity [30,32–36]. However, reactions of atomic hydrogen with strained Si—O bonds have not been investigated theoretically, except in [32], and the perception that atomic hydrogen interacts only weakly with the silica network still prevails in the literature [1,7,37].

Drawing together the ideas of reactivity of strained Si—O bonds and the significance of atomic H in technological applications of *a*-SiO₂, in this Letter we use atomistic simulations and *ab initio* calculations to demonstrate that atomic hydrogen can indeed break strained Si—O bonds in nondefective *a*-SiO₂ networks, generating a threefold-coordinated Si dangling bond facing a hydroxyl O-H group

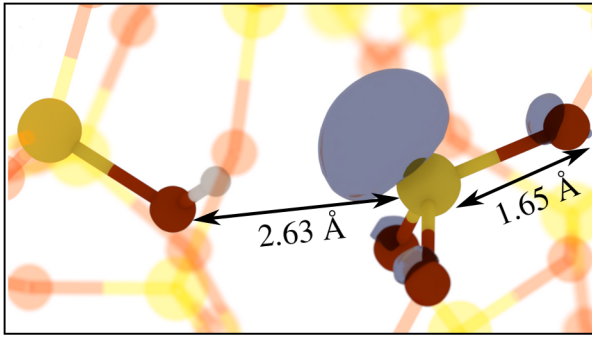


FIG. 1 (color online). Atomic configuration and spin density of the hydrogen-induced defect: the hydroxyl E' center. The Si atoms are the bigger yellow balls, the O atoms are the smaller red balls and the H atom is the small white ball. The spin density is the blue, transparent polyhedron. It is clearly localized on the threefold-coordinated Si and its three O neighbors which faces a hydroxyl group.

which we refer to as the hydroxyl E' center [see Fig. 1]. The structural disorder which results in the presence of strained Si—O bonds makes the revealed mechanism pertinent to defect generation in complex silicate glasses, natural minerals, and tectosilicate materials in general.

To model a -SiO₂ and obtain a distribution of defect properties, the REAXFF [38,39] force-field—implemented in the LAMMPS code [40]—was used to generate 116 periodic models of a -SiO₂, each containing 216 atoms. We used classical molecular dynamics and a melt and quench procedure described in detail in Ref. [36]. Densities of the REAXFF a -SiO₂ structures ranged from 1.99 to 2.27 g cm⁻³, averaging at 2.16 g cm⁻³. These values fall within the range of densities known for a -SiO₂. The distributions of Si—O bonds and Si-O-Si angles in our samples are described in detail in Ref. [36] and agree well with previous calculations by other authors [41]. We have calculated the neutron structure factors for our models and they show excellent agreement with experiment [42], indicating that our models describe both the short- and long-range order and are indeed representative of a -SiO₂.

Density functional theory (DFT), implemented in the CP2K code [43], was used to further optimize the geometries of amorphous structures and calculate their electronic structures. The nonlocal functional PBE0_TC_LRC was used in all calculations with a cutoff radius of 2.0 Å for the truncated Coulomb operator [44]. Inclusion of Hartree-Fock exchange provides an accurate description of the band gap and localized states that may be involved in the charge trapping processes. The CP2K code uses a Gaussian basis set with an auxiliary plane-wave basis set [45]. We employed a double- ζ basis set with polarization functions [46] for all atoms in conjunction with the Goedecker-Teter-Hutter (GTH) pseudopotential [47]. Calculating hyperfine interactions necessitated the use of all electron basis sets using the Gaussian and augmented plane-wave (GAPW)

approach. Basis sets with contraction schemes of (8831/831/1),(8411/411/11), and 6-311G** were used for silicon [48], oxygen [49], and H [50], respectively. The plane wave cutoff was set to 5440 eV (400 Ry). To reduce the computational cost of nonlocal functional calculations, the auxiliary density matrix method (ADMM) was employed [51]. The density is mapped onto a much sparser Gaussian basis set containing less diffuse and fewer primitive Gaussian functions than the one employed in the rest of the calculation. All geometry optimizations were performed using the Broyden-Fletcher-Goldfarb-Shanno (BFGS) optimizer to minimize forces on atoms to within 37 pN (2.3×10^{-2} eV Å⁻¹). Cell vectors were not allowed to relax. Barriers between configurations were calculated using the climbing-image nudged-elastic-band method (CI-NEB) [52]. Linear interpolation was used to generate 10 images to be optimized, with each of the images connected by a spring with a force constant of 2 eV Å².

Initially, we investigated interstitial H⁰ atoms in a -SiO₂; following suggestions by previous studies [7], we first placed a single H atom in random positions in our a -SiO₂ samples under the constraint that it is further than 2 Å away from its nearest neighbor [37,53]. Minimizing the total energy of 26 independent samples with respect to the atomic coordinates shows that in these positions the interstitial H atom only weakly interacts with the a -SiO₂ network, with the nearest neighbors found at ≈ 2.6 Å. The spin density is almost entirely localized on the H atom and a one-electron level is located in the a -SiO₂ band gap at 0.7 eV on average above the valence band, in accord with previous studies [53]. Similarly, H₂ molecules prefer locations in the middle of voids in our a -SiO₂ structures and interact negligibly with the matrix, again in good agreement with previous calculations [37,54].

Investigating whether H⁰ can bind more strongly in the a -SiO₂ matrix is complicated by the structural disorder. To find possible binding configurations, we placed H atoms randomly at 1.0 Å away from O atoms, i.e., within the typical O-H bond length. These calculations resulted in several types of stable configurations. Formation energies of these configurations are distributed over a wide range, but in what is by far the lowest energy configuration, the H atom invariably breaks an Si—O bond forming a new defect which is the main focus of this Letter and is shown in Fig. 1. This configuration resembles an E' center perturbed by a nascent OH group, and shall be referred to as a hydroxyl E' center. The other configurations are discussed in detail in Ref. [55]. We found that the hydroxyl E' center always formed when H⁰ was bound to strained Si—O bonds longer than 1.65 Å in all 116 different nondefective a -SiO₂ samples. The concentration of such bonds in our samples is 2.2%. The barrier for an interstitial H⁰ to break such a Si—O bond and form this center calculated from 13 different models averages 1.0 eV, ranging between 0.5 and 1.3 eV. Although we observe that this barrier has a trend to reduce

in the case of longer Si—O bonds, finding the full range of such barriers in our samples proved computationally unfeasible.

As mentioned earlier, the hydroxyl E' center is the lowest energy hydrogenic interaction we found, 0.8 eV lower on average than that of an interstitial H^0 in the SiO_2 network. It shows a wide distribution of energy differences, ranging between 0.3 and 2.3 eV lower than the energy of interstitial H^0 . We note that in perfect wide-gap crystalline oxides, including α quartz, interstitial H^0 behaves as a negative U center; it is thermodynamically unstable in the neutral charge state, preferring to convert into H^+ or H^- depending on the position of the Fermi level [1–4,6]. Further studies also demonstrated that interstitial H^0 behaves as a negative U center in α - SiO_2 [7]. In a separate paper [55], we demonstrate that some hydroxyl E' centers retain the negative U behavior, but a significant part of the neutral hydroxyl E' centers in our samples prove to be the most thermodynamically stable hydrogenic state across a wide range of Fermi levels. When the Si/ SiO_2 band offset is taken into account, some configurations were found to be stable across the entire Si band gap, making the neutral hydroxyl E' center a thermodynamically dominant defect in an Si/ SiO_2 system.

The Si facing the hydroxyl group in the hydroxyl E' center is threefold-coordinated with an electron residing on it. The unpaired spin is strongly localized on the Si atom with an average Mulliken spin moment of 0.90, ranging from 0.84 to 0.98. The calculated average values of hyperfine splitting on Si, the nearest neighbor O ions and H of the O-H group are 48.4, 3.0, and 0.1 mT, respectively. We note that the hydroxyl E' center may be equivalent to the $E'(\text{OH})$ center proposed in [30] as both centers have very similar hyperfine splittings on the H atom. However, our calculations demonstrate a wider spread of H hyperfine values (0.05–0.15 mT) due to the mobility of the O-H group [see Fig. 2(a)].

The Si—O bonds of the $\text{O}_3 \equiv \text{Si}$ moiety in the hydroxyl E' center average at 1.65 Å (from the 116 independent configurations considered) while the distance between the dissociated Si and O atoms [see Fig. 1] averages at 2.63 Å exhibiting a wide distribution, shown in Fig. 2(a). The position of the one-electron defect level with respect to the top of the valence band correlates with the nonbonding Si-O distance, shown in Fig. 2(b). The average position of the one-electron level is about 3.1 eV above the α - SiO_2 valence band. The further away the Si and the negative O ion are from each other, the deeper (closer to the top of the valence band) the defect level becomes as this reduces the repulsion between the unpaired electron and the O ion. This reduction in repulsion energy also increases the relative stability of the hydroxyl E' center with respect to the H interstitial atom, as seen in Fig. 2(c).

The hydroxyl E' center can take part in several further reactions involving hydrogen atoms and molecules, as

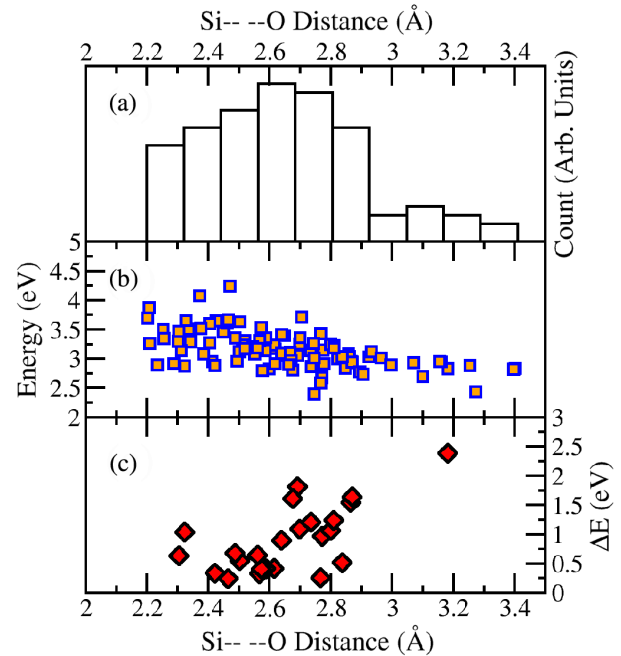
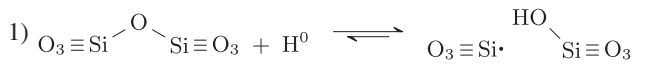
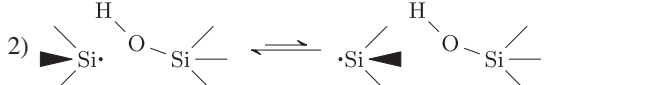
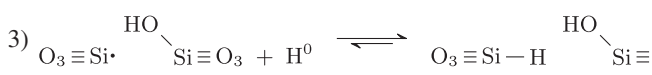
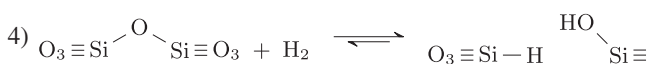


FIG. 2 (color online). Correlations between the one-electron levels and relative stabilities of the hydroxyl E' center with the nonbonding Si-O interaction. (a) A histogram of the distribution of the Si-O distances of the dissociated Si—O bond in the hydroxyl E' center [see Fig. 1]; (b) energies of the one-electron defect levels with respect to the top of the α - SiO_2 valence band plotted against the Si-O distance; (c) the relative stability of the hydroxyl E' with respect to an interstitial H atom, plotted against the Si-O distance.

summarized in Table I. Reaction 2 corresponds to the formation of a second, so called back-projected, isomer of the hydroxyl E' center. In this reaction, the Si dangling bond moves through the plane of its three O neighbors forming a stable state where the Si is inverted with respect to the original configuration. This requires overcoming a significant energy barrier of 1.8 eV [see reaction 2 in Table I], but creates a defect configuration with an unpaired electron now facing away from the Si-O-H group. The local geometry of this back-projected configuration is rather similar to the original configuration, but the distance between the threefold-coordinated Si and the hydroxyl group increases to an average of 3.43 Å. We find that the original configuration is on average 0.7 eV more stable than this back-projected configuration. Although the activation energy for this reaction is rather high, we note that the bistability of this defect is consistent with a characteristic of defects suspected in electronic device reliability issues [56].

Reaction 3 corresponds to the barrier-less passivation of the hydroxyl E' center by atomic hydrogen. The calculated binding energy of the Si-H bond that is formed after passivation averages at 4.2 eV from 13 systems, ranging from 4.0 to 4.3 eV. The length of the Si-H bonds in α - SiO_2 has a very narrow distribution in contrast to those

TABLE I. The calculated reaction barriers and relative energies (in eV) of hydrogen interactions with the α -SiO₂ matrix. ΔE is the total energy difference between the left- and right-hand sides of each reaction. (1) H atom attacking a bridging O to produce the hydroxyl E' center. (2) Relaxation of Si dangling bond through the plane of its neighbors to form the back-projected configuration. (3) Atomic H passivating the hydroxyl E' center. (4) H₂ molecule attacking a bridging O to make the passivated configuration of the hydroxyl E' center. The shorter arrow corresponds to lower reaction barriers.

Reaction	Forward reactions			Reverse reactions			ΔE
	Minimum	Maximum	Average	Minimum	Maximum	Average	
1) 	0.50	1.71	0.91	1.25	2.40	1.66	-0.75
2) 	1.00	2.34	1.75	0.31	1.89	1.08	0.67
3) 	0.00	0.00	0.00	3.96	4.31	4.19	-4.19
4) 	1.07	2.15	1.74	1.57	2.45	1.94	-0.20

associated with the Si and O atoms, in agreement with the common perception that the Si-H bond is very stable and hence the passivation is very effective. The barrier for the depassivation, the reverse of reaction 3, in this case, is about 4.2 eV, i.e., the strength of the Si-H bond. Passivation of the hydroxyl E' center eliminates the defect levels in the α -SiO₂ band gap.

We note that the same passivated defect state can be created via dissociation of an H₂ molecule at a strained Si—O bond in the α -SiO₂ network (reaction 4 in Table I). Although the passivated state is on average more stable than an interstitial H₂ molecule, the barriers for both the forward and reverse reactions are much higher because they both require rupture of strong bonds: H-H (forward) or Si-H/O-H (reverse). These results suggest that the concentration of hydroxyl E' centers strongly depends on the sample history and the concentration of molecular and atomic hydrogen during thermal treatment of α -SiO₂.

To summarize, our results clearly demonstrate that the presence of strained Si—O bonds in α -SiO₂ gives rise to an additional channel of interaction of H atoms with α -SiO₂ networks, predicting the formation of a hydroxyl E' center. Hence, H⁰ is not always a benign agent in defect-free α -SiO₂ networks and can produce thermodynamically stable neutral defects in α -SiO₂, adding to the density of dangling bond defects, such as E' centers, which are implicated in reliability issues of devices which utilize α -SiO₂. With the current trend in technology to lower fabrication processing temperatures, extreme bonding geometries in the oxide are expected to become more abundant and increase the influence of strain, ranging from ultrathin oxides sandwiched between electrodes to porous low- k insulators intrinsically strained by rebonding reactions. Hence, this discovery of unexpected reactivity of atomic hydrogen may have significant implications for the

future of silica based device processing. It may also shed new light on the behavior of atomic hydrogen in other amorphous solids, in which H⁰ is thought to interact negligibly [1], as well as on the so-called hydrogen spillover [57]. Moreover, it has recently been reported by many researchers that application of catalytic metal electrodes such as Pt [58], Pd [59], or Ru [60], in combination with annealing in a H-containing ambient allows one to improve the electrical properties of a wide range of device structures. This observation points towards the effect(s) of atomic H; since the reversible behavior expected for the classical passivation-depassivation scheme is not reported, the most plausible explanation is the interaction of hydrogen with amorphous interlayers or grain boundaries in a way similar to the mechanism described here for α -SiO₂.

The authors acknowledge EPSRC and the EU FP7 project MORDRED (EU Project Grant No. 261868) and COST Action CM1104 for financial support. We would like to thank the UK's HPC Materials Chemistry Consortium, which is funded by EPSRC (EP/F067496), for providing computer resources on the UK's national high-performance computing service HECToR and Archer. The authors are grateful to L. Skuja, Y. Wimmer, W. Goes, F. Schanovsky, and G. Pobegen for valuable and stimulating discussions.

*al-moatasem.el-sayed.10@ucl.ac.uk

†matthew.watkins@ucl.ac.uk

‡grasser@iue.tuwien.ac.at

§valeri.afanasiev@fys.kuleuven.be

¶a.shluger@ucl.ac.uk

[1] H. Li and J. Robertson, *J. Appl. Phys.* **115**, 203708 (2014).

- [2] C. Van de Walle and J. Neugebauer, *Nature (London)* **423**, 626 (2003).
- [3] G. H. Enevoldsen, H. P. Pinto, A. S. Foster, M. C. R. Jensen, W. A. Hofer, B. Hammer, J. V. Lauritsen, and F. Besenbacher, *Phys. Rev. Lett.* **102**, 136103 (2009).
- [4] K. Kajihara, L. Skuja, M. Hirano, and H. Hosono, *Phys. Rev. Lett.* **89**, 135507 (2002).
- [5] K. Kajihara, L. Skuja, M. Hirano, and H. Hosono, *Phys. Rev. B* **74**, 094202 (2006).
- [6] D. M. Hofmann, A. Hofstaetter, F. Leiter, H. Zhou, F. Henecker, B. K. Meyer, S. B. Orlinskii, J. Schmidt, and P. G. Baranov, *Phys. Rev. Lett.* **88**, 045504 (2002).
- [7] J. Godet and A. Pasquarello, *Microelectron. Eng.* **80**, 288 (2005).
- [8] B. E. Hobbs, *Point Defects in Minerals* (American Geophysical Union, Washington, DC, 1985), p. 151.
- [9] D. L. Griscom, *Nucl. Instrum. Methods Phys. Res., Sect. B* **46**, 12 (1990).
- [10] A. G. Revesz, *IEEE Trans. Nucl. Sci.* **24**, 2102 (1977).
- [11] F. B. McLean, *IEEE Trans. Nucl. Sci.* **27**, 1651 (1980).
- [12] D. L. Griscom, *J. Appl. Phys.* **58**, 2524 (1985).
- [13] D. J. DiMaria, E. Cartier, and D. Arnold, *J. Appl. Phys.* **73**, 3367 (1993).
- [14] C. R. Helms and E. H. Poindexter, *Rep. Prog. Phys.* **57**, 791 (1994).
- [15] G. Pobegen, T. Aichinger, and M. Nelhiebel, Impact of Hydrogen on the Bias Temperature Instability, in *Bias Temperature Instability for Devices and Circuits*, edited by T. Grassler (Springer, New York, 2014), p. 485.
- [16] M. Wilde, M. Matsumoto, and K. Fukutani, *J. Appl. Phys.* **92**, 4320 (2002).
- [17] V. V. Afanas'ev, J. M. M. de Nijs, P. Balk, and A. Stesmans, *J. Appl. Phys.* **78**, 6481 (1995).
- [18] A. Stesmans and V. V. Afanas'ev, *Appl. Phys. Lett.* **72**, 2271 (1998).
- [19] V. V. Afanas'ev and A. Stesmans, *J. Electrochem. Soc.* **148**, G279 (2001).
- [20] M. Wilde and K. Fukutani, *Surf. Sci. Rep.* **69**, 196 (2014).
- [21] A. Rivera, A. van Veen, H. Schut, J. M. M. de Nijs, and P. Balk, *Solid State Electron.* **46**, 1775 (2002).
- [22] R. A. B. Devine, W. L. Warren, J. B. Xu, I. H. Wilson, P. Paillet, and J. L. Leray, *J. Appl. Phys.* **77**, 175 (1995).
- [23] R. A. B. Devine, D. Mathiot, W. L. Warren, and B. Aspar, *J. Appl. Phys.* **79**, 2302 (1996).
- [24] V. V. Afanas'ev and A. Stesmans, *Phys. Rev. B* **60**, 5506 (1999).
- [25] V. V. Afanas'ev, F. Ciobanu, G. Pensl, and A. Stesmans, *Solid State Electron.* **46**, 1815 (2002).
- [26] V. Afanas'ev and A. Stesmans, *Europhys. Lett.* **53**, 233 (2001).
- [27] V. V. Afanas'ev and A. Stesmans, *Phys. Rev. Lett.* **78**, 2437 (1997).
- [28] J. Vitko, *J. Appl. Phys.* **49**, 5530 (1978).
- [29] V. A. Radzig, *Kinet. Katal.* **20**, 456 (1979).
- [30] L. Skuja, K. Kajihara, M. Hirano, A. Saitoh, and H. Hosono, *J. Non-Cryst. Solids* **352**, 2297 (2006).
- [31] L. Skuja, K. Kajihara, and H. Hirano, and M. Hosono, *Nucl. Instrum. Methods Phys. Res., Sect. B* **266**, 2971 (2008).
- [32] A. H. Edwards and G. Germann, *Nucl. Instrum. Methods Phys. Res., Sect. B* **32**, 238 (1988).
- [33] K. Awazu and H. Kawazoe, *J. Appl. Phys.* **94**, 6243 (2003).
- [34] R. Devine, *Nucl. Instrum. Methods Phys. Res., Sect. B* **91**, 378 (1994).
- [35] H. Hosono, Y. Ikuta, T. Kinoshita, K. Kajihara, and M. Hirano, *Phys. Rev. Lett.* **87**, 175501 (2001).
- [36] A.-M. El-Sayed, M. B. Watkins, V. V. Afanas'ev, and A. L. Shluger, *Phys. Rev. B* **89**, 125201 (2014).
- [37] P. E. Blöchl, *Phys. Rev. B* **62**, 6158 (2000).
- [38] A. C. T. van Duin, A. Strachan, S. Stewman, Q. Zhang, X. Xu, and W. Goddard, *J. Phys. Chem. A* **107**, 3803 (2003).
- [39] J. C. Fogarty, H. M. Aktulga, A. Y. Grama, A. C. T. van Duin, and S. A. Pandit, *J. Chem. Phys.* **132**, 174704 (2010).
- [40] S. Plimpton, *J. Comput. Phys.* **117**, 1 (1995).
- [41] K. Vollmayr, W. Kob, and K. Binder, *Phys. Rev. B* **54**, 15808 (1996).
- [42] S. Susman, K. J. Volin, D. L. Price, M. Grimsditch, J. P. Rino, R. K. Kalia, P. Vashishta, G. Gwanmesia, Y. Wang, and R. C. Liebermann, *Phys. Rev. B* **43**, 1194 (1991).
- [43] J. VandeVondele, M. Krack, F. Mohamed, M. Parrinello, T. Chassaing, and J. Hutter, *Comput. Phys. Commun.* **167**, 103 (2005).
- [44] M. Guidon, J. Hutter, and J. VandeVondele, *J. Chem. Theory Comput.* **5**, 3010 (2009).
- [45] G. Lippert, J. Hutter, and M. Parrinello, *Mol. Phys.* **92**, 477 (1997).
- [46] J. VandeVondele and J. Hutter, *J. Chem. Phys.* **127**, 114105 (2007).
- [47] S. Goedecker, M. Teter, and J. Hutter, *Phys. Rev. B* **54**, 1703 (1996).
- [48] B. Civalleri and P. Ugliengo, *J. Phys. Chem. B* **104**, 9491 (2000).
- [49] M. D. Towler, N. L. Allan, N. M. Harrison, V. R. Saunders, W. C. Mackrodt, and E. Apra, *Phys. Rev. B* **50**, 5041 (1994).
- [50] R. Krishnan, J. S. Binkley, R. Seeger, and J. A. Pople, *J. Chem. Phys.* **72**, 650 (1980).
- [51] M. Guidon, J. Hutter, and J. VandeVondele, *J. Chem. Theory Comput.* **6**, 2348 (2010).
- [52] G. Henkelman, B. P. Uberuaga, and H. Jansson, *J. Chem. Phys.* **113**, 9901 (2000).
- [53] A. Yokozawa and Y. Miyamoto, *Phys. Rev. B* **55**, 13783 (1997).
- [54] P. Bunson, M. D. Ventra, S. Pantelides, R. Schrimpf, and K. Galloway, *IEEE Trans. Nucl. Sci.* **46**, 1568 (1999).
- [55] A.-M. El-Sayed, Y. Wimmer, W. Goes, T. Grassler, and A. Shluger (to be published).
- [56] F. Schanovsky, W. Gös, and T. Grassler, *J. Comput. Electron.* **9**, 135 (2010).
- [57] R. Prins, *Chem. Rev.* **112**, 2714 (2012).
- [58] Y. Hwang, R. Engel-Herbert, N. G. Rudawski, and S. Stemmer, *J. Appl. Phys.* **108**, 034111 (2010).
- [59] C. H. Wang, S. W. Wang, G. Dornboos, G. Astromskas, K. Bhuiwarka, R. Cortreras-Guerro, M. Edirisooriya, J. S. Roijas-Ramirez, G. Vellitantis, R. Oxland, M. C. Holland, C. H. Hsieh, P. Ramwall, E. Lind, W. C. Hsu, L.-E. Wernersson, R. Droopad, M. Passlack, and C. H. Diaz, *Appl. Phys. Lett.* **103**, 143510 (2013).
- [60] J. Swerts, M. Popovici, B. Kaczer, M. Aoulaiche, A. Redolfi, S. Clima, C. Caillat, W. C. Wang, V. V. Afanas'ev, N. Jourdan, C. Olk, H. Hody, S. Van Elshocht, and M. Jurczak, *IEEE Electron Device Lett.* **35**, 753 (2014).